Global Biogeochemical Cycles

Supporting Information for

Biological production, export efficiency, and phytoplankton communities across 8000 km of the South Atlantic: Basin scale similarity with mesoscale variability

E.M. Howard[1,2], C.A.Durkin[3], G.M.M. Hennon[4], F. Ribalet[5], and R.H.R. Stanley[6]

[1]Massachusetts Institute of Technology, [2]Woods Hole Oceanographic Institution, [3]Moss Landing Marine Laboratories, [4]Lamont-Doherty Earth Observatory, [5]University of Washington, [6]Wellesley College

Contents of this file

Additional Supporting Information (Files uploaded separately)

Introduction

The supporting information presented here includes a derivation of equations for correcting net community production and gross primary production for diapycnal mixing and entrainment (Text S1), as well as a discussion of potential sources of systematic errors to these rates in this and other works that are not addressed in the main text (Text S2), and criteria for excluding two rates from the analysis (Text S3). Additionally, supporting figures referred to in the this document and the main text are included. Finally, large tables that serve as supporting information to the main text are separately uploaded, but captioned in this document. All data in these tables was collected as part of the study described in the main text. Isotope data (Table S1) was analyzed as described in the main text and processed using Access software (2013, Microsoft, Redmond, WA). All other data was processed using Matlab software (release 2015b, The Mathworks, Natick, MA).

Text S1. Derivation of mixing corrections to gross primary production and net community production

Nicholson et al. 2014 derive mixing corrections for gross primary production to account for entrainment in their supplementary material. Their equation S7 is reproduced here, with measured $^{17}O/^{16}O$ and $^{18}O/^{16}O$ ratios notated as ^{17}X and ^{18}X as in the main text of this work, and the subscript *d* indicating the measured value of a property at some depth below the mixed layer:

$$C_{GPP} = \left(\frac{\partial z}{\partial t}\right)\left(\left[\frac{1}{^{17}X}\left(^{17}O_{2\,d} - {}^{17}O_2\right) - \left(O_{2\,d} - O_2\right)\right] - \lambda\left[\frac{1}{^{18}X}\left(^{18}O_{2\,d} - {}^{18}O_2\right)\left(O_{2\,d} - O_2\right)\right]\right) \quad \text{(S1)}$$

As the measured oxygen concentrations are in molal units, Eq. S1 is multiplied by the density of seawater, ρ_{sw}. If Eq. S1 is distributed, it becomes:

$$C_{GPP} = \left(\frac{\partial z}{\partial t}\right)\left(\left[\frac{^{17}O_{2\,d}}{^{17}X} - \frac{^{17}O_2}{^{17}X} - O_{2\,d} + O_2\right] - \lambda\left[\frac{^{18}O_{2\,d}}{^{18}X} - \frac{^{18}O_2}{^{18}X} - O_{2\,d} + O_2\right]\right)\rho_{sw} \quad \text{(S2)}$$

Using the definitions of ^{17}X and ^{18}X, the second term in each of the bracketed expressions simplifies to O_2, and the surface concentration of bulk oxygen cancels out of the expression:

$$C_{GPP} = \left(\frac{\partial z}{\partial t}\right)\left(\left[\frac{^{17}O_{2\,d}}{^{17}X} - O_{2\,d}\right] - \lambda\left[\frac{^{18}O_{2\,d}}{^{18}X} - O_{2\,d}\right]\right)\rho_{sw} \quad \text{(S3)}$$

Finally, the first term in each of the bracketed expressions can be multiplied by O_{2d}/O_{2d} in order to rewrite the concentrations of the rare isotopologues in terms of ^{17}X and ^{18}X, and the common factor of O_{2d} removed from all the terms within the parentheses. This leaves Eq. S4 in terms of only measured variables.

$$C_{GPP} = \left(\frac{\partial z}{\partial t}\right)O_{2\,d}\left(\left[\frac{^{17}X_d}{^{17}X} - 1\right] - \lambda\left[\frac{^{18}X_d}{^{18}X} - 1\right]\right)\rho_{sw} \quad \text{(S4)}$$

The equation for correcting for vertical diffusivity is identical to that for entrainment except that the mixing rate is equal to the vertical diffusivity coefficient K_z over the change in depth. Thus mixing from entrainment and vertical diffusivity can be combined into a single expression, Eq. S5 which is identical to Eq. 4 in the main text ($\partial z/\partial t$ set to o for shoaling):

$$C_{\mathrm{GPP}} = \left(\frac{\partial z}{\partial t} + \frac{Kz}{(z_d - z)}\right)O_{2\,d}\left(\left[\frac{^{17}X_d}{^{17}X} - 1\right] - \lambda\left[\frac{^{18}X_d}{^{18}X} - 1\right]\right)\rho_{sw} \quad \text{(S5)}$$

By similar reasoning net community production may be approximated as a function of the difference between the net biological oxygen production signal at depth and in the surface:

$$C_{\mathrm{NCP}} = \left(\frac{\partial z}{\partial t} + \frac{Kz}{(z_d - z)}\right)\left(O_{2\,\mathrm{sat_d}}\left[\frac{\Delta O_2}{Ar}\right]_d\left[\frac{Ar}{Ar_{sat}}\right]_d - O_{2\,\mathrm{sat}}\left[\frac{\Delta O_2}{Ar}\right]\left[\frac{Ar}{Ar_{sat}}\right]\right)\rho_{sw} \quad \text{(S6)}$$

This form is convenient because it expresses the components of the correction in the same form as the gas exchange term. However the biological oxygen supersaturation ($\Delta O_2/Ar$) is not mixed conservatively. The exact form can be derived by combining the separate mass balances for oxygen and argon. For the entrainment term only:

$$C_{O_2} = \left(\frac{\partial z}{\partial t}\right)\left(O_{2\,d} - O_2\right)\rho_{sw} \quad \text{(S7)}$$

$$C_{Ar} = \left(\frac{\partial z}{\partial t}\right)\left(Ar_d - Ar\right)\rho_{sw} \quad \text{(S8)}$$

Multiplying Eq. S8 by $O_{2\,sat}/Ar_{sat}$, subtracting from Eq. S7, and multiplying the resulting mass balance by $O_{2\,sat}/O_{2\,sat}$ in identical manner to the derivation of the net community production expression in *Howard et al.* [2011] leads to the following expression (Eq. 3 in main text):

$$C_{\mathrm{NCP,exact}} = \left(\frac{\partial z}{\partial t}\right)\left(O_{2\,\mathrm{sat}}\left[\frac{O_{2\,d} - O_2}{O_{2\,\mathrm{sat}}} - \frac{Ar_d - Ar}{Ar_{sat}}\right]\right)\rho_{sw} \quad \text{(S9)}$$

The approximate expression in Eq. S6 can be rewritten in the same form as Eq. S9 by substituting the definition of $\Delta O_2/Ar$, multiplying by $O_{2\,sat}/O_{2\,sat}$ and Ar_{sat}/Ar_{sat} where appropriate and cancelling terms:

$$C_{\mathrm{NCP}} = \left(\frac{\partial z}{\partial t}\right)\left(\mathrm{O}_{2\ \mathrm{sat_d}}\left[\frac{\mathrm{O}_{2\ \mathrm{d}}/\mathrm{Ar_d}}{\mathrm{O}_{2\ \mathrm{sat\ d}}/\mathrm{Ar}_{\mathrm{sat\ d}}} - 1\right]\left[\frac{\mathrm{Ar}}{\mathrm{Ar}_{\mathrm{sat}}}\right]_{\mathrm{d}} - \mathrm{O}_{2\ \mathrm{sat}}\left[\frac{\mathrm{O}_2/\mathrm{Ar}}{\mathrm{O}_{2\ \mathrm{sat}}/\mathrm{Ar}_{\mathrm{sat}}} - 1\right]\left[\frac{\mathrm{Ar}}{\mathrm{Ar}_{\mathrm{sat}}}\right]\right)\rho_{\mathrm{sw}} \quad \text{(S10)}$$

$$C_{\mathrm{NCP}} = \left(\frac{\partial z}{\partial t}\right)\left(\mathrm{O}_{2\ \mathrm{d}} - \mathrm{O}_{2\ \mathrm{sat_d}}\left[\frac{\mathrm{Ar}}{\mathrm{Ar}_{\mathrm{sat}}}\right]_{\mathrm{d}} - \mathrm{O}_2 + \mathrm{O}_{2\ \mathrm{sat}}\left[\frac{\mathrm{Ar}}{\mathrm{Ar}_{\mathrm{sat}}}\right]\right)\rho_{\mathrm{sw}} \quad \text{(S11)}$$

$$C_{\mathrm{NCP}} = \left(\frac{\partial z}{\partial t}\right)\left(\mathrm{O}_{2\ \mathrm{sat}}\left[\frac{\mathrm{O}_{2\ \mathrm{d}} - \mathrm{O}_2}{\mathrm{O}_{2\ \mathrm{sat}}} - \frac{\left(\frac{\mathrm{O}_2/\mathrm{Ar}_{\mathrm{sat\ d}}}{\mathrm{O}_2/\mathrm{Ar}_{\mathrm{sat}}}\right)\mathrm{Ar}_{\mathrm{d}} - \mathrm{Ar}}{\mathrm{Ar}_{\mathrm{sat}}}\right]\right)\rho_{\mathrm{sw}} \quad \text{(S12)}$$

Thus the approximate form adds a factor to the argon concentration at depth that is close to one, as the saturation ratio of oxygen to argon stays relatively constant with depth; the solubility functions of oxygen and argon are very similar. The approximate expression (Eqs. S6 or S12) is within 0.15 mmol m^{-2} d^{-1} of the exact expression in all cases in this dataset (< 1% relative standard error except when net community production is very close to zero) and is an acceptable formulation in most situations.

Text S2. Sources of systematic bias in oxygen tracer mass balances

We present some important additional considerations related to the calculation of net community production (NCP) and gross primary production (GPP) using the O_2/Ar and triple oxygen isotope tracers. First, we address the probable biases in the gas mass balances used in this paper. Next we note how diel biological cycles influence uncertainty in NCP and GPP, and finally the role of argon saturation state in the calculation of NCP. These important caveats may have implications for the use of oxygen to argon and triple oxygen isotope ratios in other work.

S2.1 Lateral advection, upwelling, and mixing

Equations 5 and 6 in the main text (NCP and GPP) ignore lateral advection, as well as the potential role of upwelling and surface divergence. While this is a reasonable assumption across the South Atlantic Gyre, with surface current velocities on the order of cm s^{-1} and low variability in the tracer values, it may not hold in the equatorial region, particularly between ~5° S and 5° N, which has complex surface and near surface zonal flows related to the North and South Equatorial Currents and Equatorial Counter Current, with velocities up to tens of cm s^{-1} [*Peterson and Stramma* 1991, *Lumpkin and Garzoli* 2005, *Brandt et al.* 2006]. In general, surface transport of the O_2/Ar and triple oxygen isotope tracers cannot be constrained because advective gradients cannot be determined at high enough resolution in this study to determine zonal flow. However, within the equatorial region the triple oxygen isotope tracer $^{17}\Delta$ does not vary between adjacent sample locations by more than twice the standard deviation of a single location. Thus differences in the tracer are driven primarily by gas exchange and vertical exchange. Gradients in ΔO_2/Ar are larger relative to uncertainties than the lateral gradients in $^{17}\Delta$, but generally the difference between stations is no larger than the standard deviation at either station. These relatively small changes over degree scales suggest that surface gradients can be neglected within the uncertainty bounds of the GPP and NCP rates: as a worst case scenario, with a 50 cm s^{-1} surface current [*Lumpkin and Garzoli* 2005], and the maximum observed gradients in the equatorial region of 15 per meg $^{17}\Delta$ over 220 km, and 1.5% ΔO_2/Ar over 145 km, and 3 µmol O_2 m^{-3} difference in surface oxygen saturation concentration over the same distance, then over the range of observed production rates GPP is altered by no more than 4% and NCP by no more than 2%.

Vertical gradients in the tracers are large compared to horizontal gradients, and upwelled water would act similarly to entrainment or mixing in decreasing surface ΔO_2/Ar and increasing $^{17}\Delta$. While upwelling was not directly evaluated in this study, it is likely minimal compared to in the Eastern Equatorial Atlantic [*Rhein et al.* 2010, *Kadko and Johns* 2011] as the cruise transect was

well west of the main upwelling region and associated surface chlorophyll *a* feature [e.g. *Grodsky et al.* 2008]. Measured rates close to our transect location are ~ 0 m d^{-1} [*Kadko and Johns* 2011] (4.7° S, 26.8° W, May 2009, error estimated from reported results as ~0.05 m d^{-1}). Satellite based divergence indicates annual minimum upwelling in March and April near our cruise track with near zero divergence to net convergence [*Helber et al.* 2007]. Thus we believe an assumption of near zero upwelling is justified for this dataset, but we recognize that such an assumption makes our GPP estimate an upper bound and our NCP estimate a lower bound.

Finally, GPP and NCP are sensitive to the vertical diffusivity coefficient, K_z, which likely varies across the South Atlantic. Increased vertical diffusivity would act to lower our GPP estimates and raise apparent NCP and the NCP/GPP ratio, as with upwelling. We choose K_z=1x10^{-5} m^2 s^{-1} (8.6x10^{-1} m^2 d^{-1}) as representative of mixing across the base of the mixed layer based on microscale measurement derived K_z by Mouriño-Carballido et al. [2011] at the same time of year (they find average K_z in the SAG and WTA of 0.3(0.5)x10^{-5} m^2 s^{-1} over the entire surface 150 m). This estimate is consistent with global values for below the mixed layer (order of 10^{-5} m^2 s^{-1}) [*Wunsch and Ferarri* 2004], diffusivity derived from thermocline argon supersaturation for decadal scale mixing in the subtropical North Pacific (no more than 2 x10^{-5} m^2 s^{-1}) [*Emerson et al.* 2012], and a tracer release experiment in the Southern Ocean (1(2)x10^{-5} m^2 s^{-1}) [*Law et al.* 2003]. In the open ocean, values up to the order of 10^{-4} m^2 s^{-1} are observed primarily in actively upwelling regions such as the Eastern Equatorial Pacific [*Carr et al.* 1992, *Haskell et al.* 2015] and Eastern Equatorial Atlantic [*Kadko and Johns* 2011, *Rhein et al.* 2010]. Our choice of K_z may not be high enough for the WTA or the more energetically mixed boundary regions such as the SST, but is a reasonable lower bound across the transect. Increasing K_z by an order of magnitude to 1x10^{-4} m^2 s^{-1} on average decreases GPP by 26%, and increases NCP and the NCP/GPP ratio by 6% and 36% respectively. If K_z is instead set to 5 or 2x10^{-5} m^2 s^{-1}, the changes in GPP, NCP, and NCP/GPP are -11%, 3%, and 12% and -3%, 1%, and 4% respectively compared to rates at K_z=1x10^{-5} m^2 s^{-1}. The sensitivity of absolute rates and NCP/GPP ratio is low except when NCP and GPP are low and of similar magnitude (primarily the SAG)—in this case the higher mixing rates (e.g. K_z greater than ~3x10^{-5} m^2 s^{-1}) may increase the NCP/GPP ratio by 0.1 or more. However, this region is also where we would expect stratification to be strongest and K_z to be most similar to the minimum bound we chose. Direct evaluation of upwelling and vertical mixing rates over a similar timescale to the oxygen based tracers would be preferable to the assumptions above; the ^{7}Be approach is a promising technique for just such an approach [*Haskell et al.* 2015, *Kadko and Johns* 2011].

S2.2 Sample time in relation to diel cycles

In principle, triple oxygen isotope and O_2/Ar derived rates of NCP and GPP integrate over the residence time of dissolved oxygen in the mixed layer, set primarily by the gas transfer coefficient and the mixed layer depth. The residence time is generally on the order of a few days to two weeks, and the tracer is expected to average sufficient time and space that diel cycles and small-scale heterogeneity in production and respiration are averaged out [*Juranek and Quay* 2013]. In practice daily and sub-daily variations in oxygen, the O_2/Ar ratio, and triple oxygen isotopes can be used to glean additional information about localized metabolic cycling [*Hamme et al.* 2012, *Ferrón et al.* 2015, *Nicholson et al.* 2015], and gas-exchange fluxes [*Sarma et al.* 2006] on shorter time scales. These daily cycles dominate the time rate of change of the tracers over seasonal cycles, and steady state solutions to GPP and NCP as were calculated in this work may be in error. $^{17}\Delta$ and ΔO_2/Ar at a single sample location (28.2° S) over one day are plotted against local time in Figure S1a. The systematic increase in the tracers until sunset and

then decrease until the following midday is likely related to the balance of diel wind and productivity cycles. Similar patterns of a diel cycle were observed at locations in each biogeographic province (not plotted). Treating the data with the standard steady-state assumption and ignoring short term variability in gas exchange and productivity results in the GPP and NCP rates in Figure S1b. In this case, a sample taken around 06:00 local time leads to estimates of GPP and NCP close to the mean rates, while rates derived from samples taken in the early evening would be 40-60% higher than those from midday samples—this range is similar to the difference between adjacent sample locations. Sample times in this dataset are roughly evenly distributed throughout the day within each region and no trends of production with time of day are observed in the overall dataset (Figure S2); time of sampling likely does not greatly bias the analysis in this work. For comparison across locations with and without time-series data, we report the location mean and standard deviation of all replicates, regardless of time of day sampled, and assume steady state in all calculations. While it may not be possible to evaluate the nominal sample time for a given location *a priori* when planning a study, if it is not possible to sample multiple timepoints within a given day it may be preferable to avoid sampling during morning and dusk—i.e. during daily periods of expected peak tracer accumulation and deficit (as suggested by Hamme et al. [2012]).

S2.3 Argon supersaturation and the calculation of net community production

Biological oxygen saturation [*Hendricks et al.* 2004] (or equivalently supersaturation, $\Delta O_2/Ar$ [*Kaiser et al.* 2005]) is defined in order to calculate NCP, often with the explicit assumption that Ar is at saturation in the absence of direct measurements of argon or oxygen concentration paired with the O_2/Ar ratio. Assuming argon is at 100% saturation is a reasonable approximation in most cases, and neglecting Ar/Ar_{sat} in the gas exchange term generally leads to small systematic errors of no more than a few percent in NCP. However, when incorporating terms for mixing, entrainment, or upwelling the gradient in Ar/Ar_{sat} may be substantial; some locations in this study have 5 to 10% supersaturation differences between the surface and below the pycnocline. With the gas exchange, entrainment and mixing in this study, setting $Ar/Ar_{sat} = 1$ leads to systematic underestimation of NCP and the NCP/GPP ratio by 3% on average (3, 5, 1, and 1% underestimation in the SST, SAG, WTA, and ARP). The underestimation at individual sample locations may be more significant however, with NCP up to 9% too low. This is similar to the systematic uncertainty associated with the choices of gas exchange parameterization (~15%) or vertical diffusivity (~up to 10% in general). Thus when including diapycnal exchange terms in the mass balance for NCP, measured argon or oxygen concentrations are preferable to assuming that argon is saturated with respect to the atmosphere when subsurface argon supersaturations are expected to be large [q.v. *Gehrie et al.* 2006].

Text S3. Specific production rates excluded

GPP rates from duplicate samples at 19.3° S and 17.0° S were excluded from the mean rates reported in Table S3. These samples were outliers in the overall dataset (more than two standard deviations below the mean for all other GPP) and relative to their paired duplicate samples (more than two standard deviations below their duplicate rates assuming the uncertainty in a typical rate, and an order of magnitude lower than the duplicates). Further, the GPP rates from these samples were biologically unlikely—within uncertainties of zero and less than the associated NCP rates from the same samples (which were in contrast similar to NCP from the duplicate samples). Such rates are not biologically feasible, implying practically no photosynthesis yet net autotrophic community metabolism (i.e. GPP-R > GPP). For these

samples only, the mixing corrections may have introduced proportionally very large biases; errors associated with the mixing correction become proportionally very large when production rates are low. Comparing GPP with and without mixing corrections (Table S2) indicates that the mixing corrections at these locations were similar in magnitude to the uncorrected rates, meaning a small bias in the mixing correction could overwhelm the actual environmental signal in the calculation of GPP. Furthermore, these were stations already identified as having potentially biased mixing corrections because of the long distances from the nearest tracer depth profiles (main text section 2.1.1). While any one of these problems would not definitely exclude these or any other sample rates from the analysis, in combination the above observations suggest that these two rates are not comparable either to other rates at the same location or to other rates across the transect, and they are excluded from further analysis.

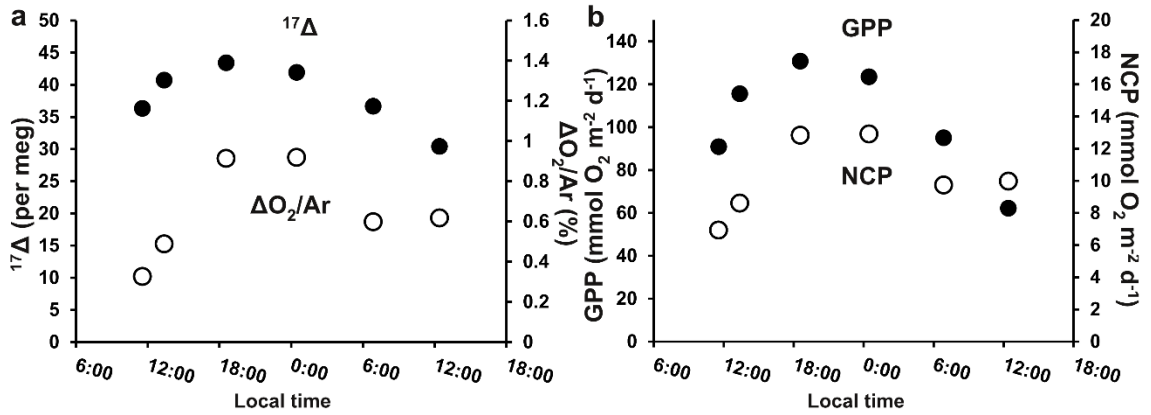

Figure S1. Underway sampling at 28.2°S relative to local noon; measured (a) the triple oxygen isotope tracer $^{17}\Delta$ and biological oxygen supersaturation $\Delta O_2/Ar$ compared to (b) gross primary production (GPP) and net community production (NCP) calculated by assuming steady state conditions and neglecting the observed time rate of change (as may be required without time-series sampling). The three quasi-Lagrangian stations (see Table S1) in the South Atlantic Gyre, Western Tropical Atlantic, and the Amazon River Plume have different timing of peak relative to minimum tracer values and day to day variability; no specific time of day is close to the mean value in all three cases and the optimal sample period for assuming steady state cannot be determined a priori in this dataset.

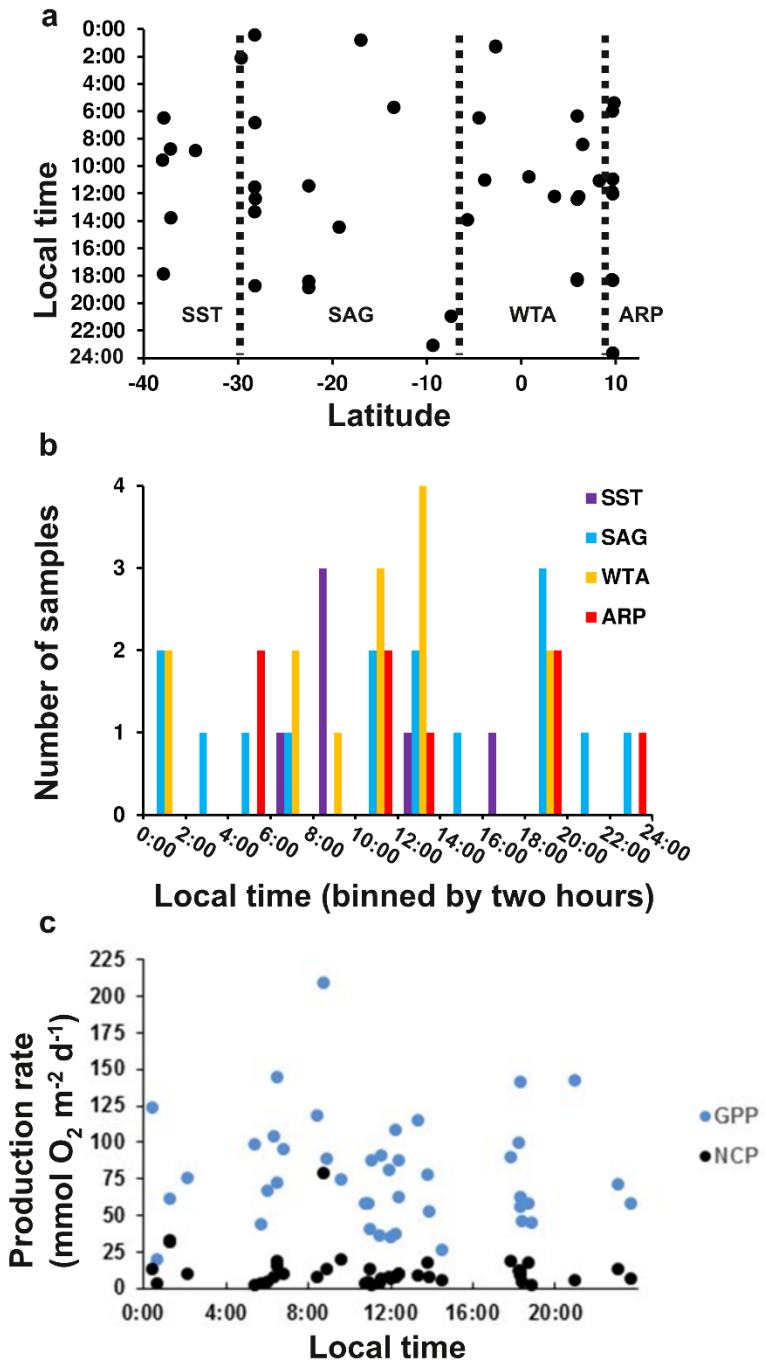

Figure S2. Gas tracer sampling time relative to local noon (**a**), number of samples in two hour time bins relative to local noon (**b**), binned by biogeographic province as defined in the text. Also, rates of GPP and NCP relative to local time (**c**). No systematic trends in sample time or production are found with respect to local time in the overall dataset, either within or between biogeographic provinces.

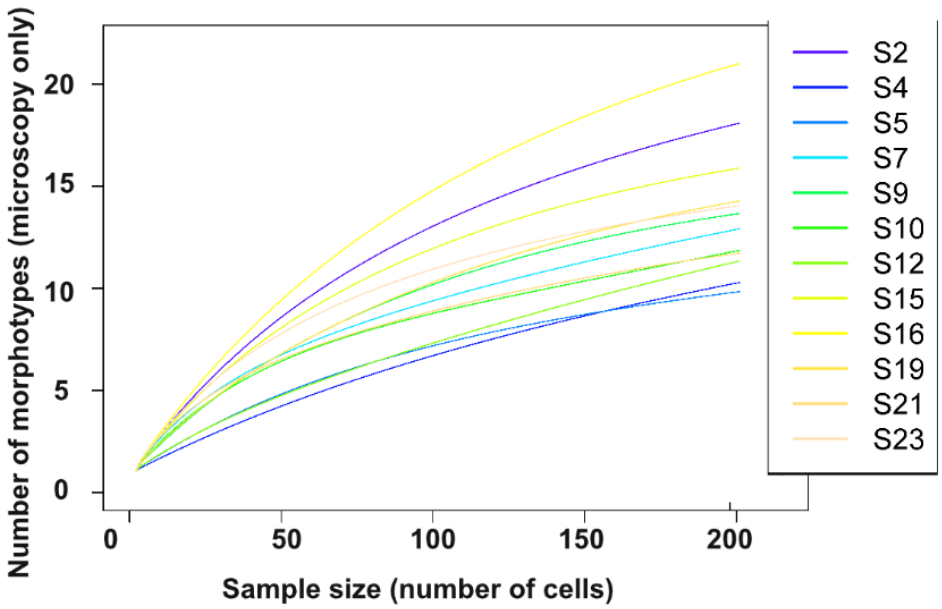

Figure S3. Rarefaction curves of number of morphotypes of microphytoplankton identified by light microscopy. Curves are identified by station number. Curves generally have not leveled out within the number of observations, indicating that not all microphytoplankton morphotypes likely to be present have been identified.

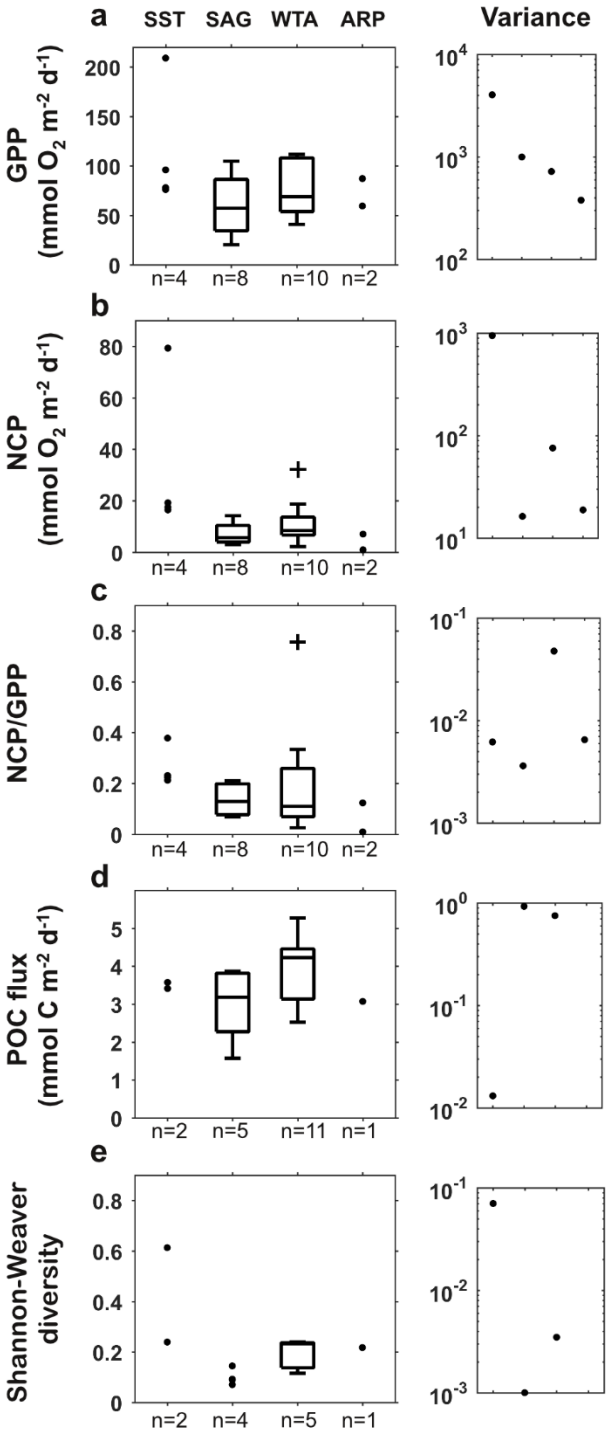

Figure S4. Selected parameters binned by biogeographic province. Individual data values are plotted for four or fewer samples in a region, and box pots for five or more samples. Potential outliers (greater than 1.5 times interquartile range from middle 50% of data) are marked as crosses on box plots. Variance (standard deviation squared) for each region is plotted in the right column. (**a**) Gross primary production, GPP, (**b**) net community production, NCP, and (**c**) the NCP/GPP ratio in the surface mixed layer. (**d**) particulate organic carbon (POC) flux at 125 m. (**e**) Shannon-Weaver diversity (H) for the phytoplankton community at 5 m.

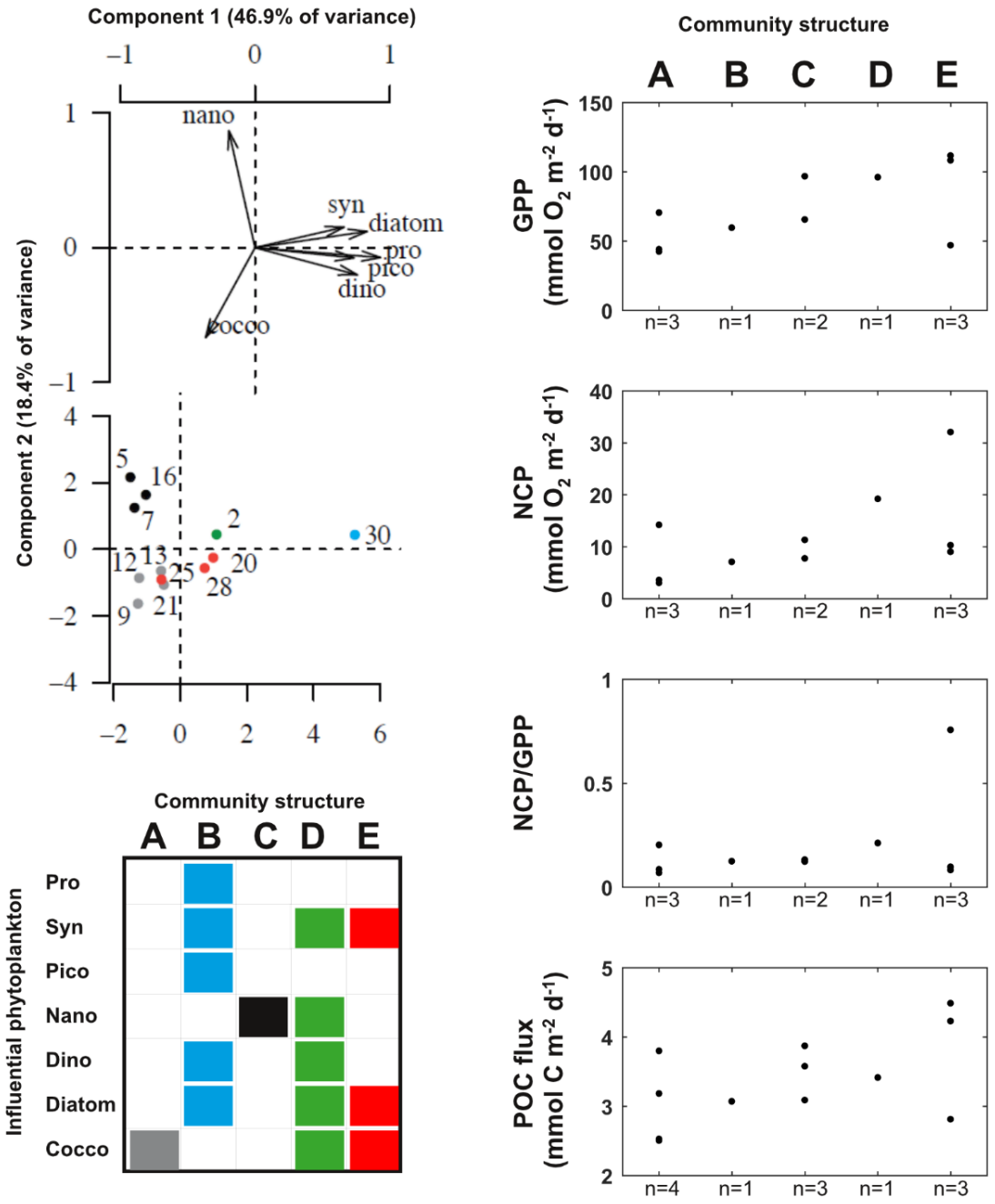

Figure S5. Results of the principal component analysis (PCA) and clustering of community structure types described in the text: (**a**) Component loadings of phytoplankton groups onto first and second components of PCA, (**b**) the component scores of each sample location in component space. Location component scores are grouped across all components of the PCA using k-means clustering to identify five community structure types (colors in panel **b**, identified in the legend, **c**). Gross primary production (GPP), net community production (NCP), the NCP/GPP ratio, and the particulate organic carbon (POC) flux are plotted for each of the location (n) to which a community structure was assigned (panels **d-g**). No significant differences in these fluxes were identified between community types.

Table S1. Sample locations and replicates with respect to biogeographic provinces. Location designations, coordinates, and sample times, along with information about the types of sampling conducted at each location.

Table S2. Isotopic results, including definitions and ancillary properties. A. Equations and definitions used in the calculation of gross primary production from the dissolved triple oxygen isotope measurements. B. Isotopic measurement information and resulting values of gross primary production and net community production for each sample, prior to averaging by location. Isotope and gas ratio definitions are defined in part A and in the main text.

Table S3. Surface results summarized by sample location. Mean values and uncertainties of all measured variables at each sample location, as well as number of replicates for each type of sample, n. Biogeographic province acronymns are South Subtropical Transition zone (SST), South Atlantic Gyre (SAG), Western Tropical Atlantic (WTA), and Amazon River Plume (ARP). Variable acronymns are gross primary production (GPP), net community production (NCP), the net community production to gross primary production ratio (NCP/GPP), Shannon-Weaver diversity (H), particulate organic carbon (POC) flux, and particulate nitrogen (PN) flux, each as defined in the text.

Table S4. Correlation matrix of mean values across transect. Correlation matrix of mean values by location for each variable, with Pearson correlation coefficients (r) shown for the upper half only of the symmetric matrix. Variables names and abbreviations are listed in boxed legend. Shaded values are significant values of r at α=0.05 ($p<0.05$). Values of p for Pearson correlation coefficient only are in parentheses for significant correlations. Boxed values are significant ($p<0.05$) using the non-parametric Spearman's rank correlation coefficeint (ρ).

Table S5. Correlation matrices of mean and variance across biogeographic provinces. Correlation matrix of mean and variance of properties binned by region, with Pearson correlation coefficients (r) shown for the upper half only of the symmetric matrix. Variables names and abbreviations are listed in boxed legend. Shaded values are significant values of r at α=0.05 ($p<0.05$). Values of p are in parentheses for significant correlations. There are too few regions to test Spearman's rank based correlation.